Title:
A human arm Proxy for testing relAtionships between muscle coNTractiOn and arm Motion In a Microgravity Environment (PANTOMIME)

Description of Project:
When performing arm-motion-related tasks under normal gravity conditions, the musculoskeletal torques, generated by contraction of numerous associated muscles, must equal those required to (1) accelerate the arm (inertial torques), (2) counteract elastic restoring forces and frictional losses in the muscle tissue, and (3) move the arm and any attached masses against the pull of gravity. In the absence of gravity, astronauts' arms performing similar tasks must generate all of the same torques except (3). Individual muscle lengths would follow identical functions of time, but the degrees of muscle contraction required would be, generally, smaller. Although electromyograms and similar devices can measure muscle activity, the true degrees of contraction of the muscles in a human during any given task are very difficult to measure. We plan to create a mechanical arm with four degrees of freedom that simulates the actual human arm as closely as possible, using elastic materials, shortened by the action of servo-motors, to model the true muscles of the arm. Via a computer interface, we propose to send time-sequences of artificial muscle contractions such that the end of the arm will execute motions that we can predict by numerical integration of the equations of motion, in the microgravity environment afforded by the NASA aircraft. We will then compare the differences between the observed and predicted motions, both in the microgravity environment and in the laboratory. We expect to learn much about how muscle contractions generate arm movements in this ambitious project, and we hope that our results may shed light on how arm-movement strategies vary between those required on earth and in the weightless environment. This project will also give us an incentive to develop a mechanical arm that we can use for further studies regarding human arm physics under normal gravity conditions.

Test Objectives

The purpose of this experiment is to observe and analyze the motion of a mechanical arm designed to approximate some of the dynamical behavior of a true human arm in a microgravity environment. Because the arm's motion will be generated by contraction of numerous elastic cords arranged such that they geometrically resemble actual muscles of the human arm, the dynamics of the arm's motion can be directly related to the commanded (and measurable) contraction of these "muscles", and we will be able to test the actual motion of the arm against the motion predicted by numerical integration of the equations of motion. Thus, our hypothesis is as follows: Given a time sequence of muscle contraction commands, we expect that the end of our mechanical arm (i.e. the hand) will follow trajectories matching those that we predict from numerical integration of the equations of motion for the system.

We have performed initial calculations demonstrating that the muscle contractions required to move an arm at typical speeds in the presence of gravity are generally over an order of magnitude larger than they would be if gravity were absent (note that in this proposal we define the degree of muscle contraction as the absolute muscle length minus resting length, where the resting length varies by the amount of contraction of the contractile component of the muscle – i.e. the sarcomeres). Thus, while we can operate and test the arm's motion in the laboratory, the degrees of muscle contraction for each muscle required to perform similar motions will be very different in the environment of the NASA aircraft, and it will be necessary to fly our experiment on the aircraft to see if predicted motions match observed motions when gravity is absent (or nearly absent).

There is also an educational objective to our proposed experiment…..Matt will fill in…

Additional objective: stimulating students' interest in technology and physics through our outreach (just make sure it doesn't copy older proposals).

Test description: overview

For our experiment we will build a mechanical arm that simulates a real human arm as closely as possible, using elastic Thera-Band® tubing to represent the major muscles responsible for arm movement (see Figure 1), attached to strong cords, representing tendons. These simulated muscle-tendon combinations (hereafter referred to as "muscle-tendons") will be attached to an actual molded model of a human skeleton, purchased from 3B Corporation or Allegro Medical company, for example. Each muscle-tendon will originate at a pulley-shaped *horn* mounted on a servo which in turn is mounted at an appropriate location on the model skeleton (see Figure 2). Rotation of the servos will shorten the effective resting lengths of the muscle-tendons by wrapping them about the

Figure 1. Elastic Theraband® tubing comes in many degrees of elasticity. Elastic strips are also available, although we do not plan to use them at present. Human skeletal hand for scale.

horn, corresponding to the contraction of sarcomeres in actual muscle tissue. As shown in Figure 2, the muscle-tendon will typically wrap around an appropriate pivot location on the skeleton, passing through a lubricated tube, representing a tendon-sheath, which is fixed to the skeletal framework. This fixed tube will ensure that the muscle-tendons do not diverge from their intended regions of contact with the skeletal structure. The other end of each muscle-tendon will be attached (i.e. "inserted") directly to the appropriate location on the skeletal structure by an eye-hook which is screwed into the bone. The proximal edges of the bones that connect at the shoulder and elbow joints of the mechanical arm will be separated by simulated bursae (sacs filled with simulated synovial fluid) and held together by the muscle-tendons themselves, as well as perhaps by additional segments of elastic tubing surrounding each joint, for added stability (see Figure 3). The motion of fluid in this joint structure will help to produce friction, a necessary addition to any musculoskeletal simulation. More significantly, friction within the lubricated tendon sheaths will also contribute to overall friction, at a rate that believe should be roughly proportional to the rate of muscle contraction.

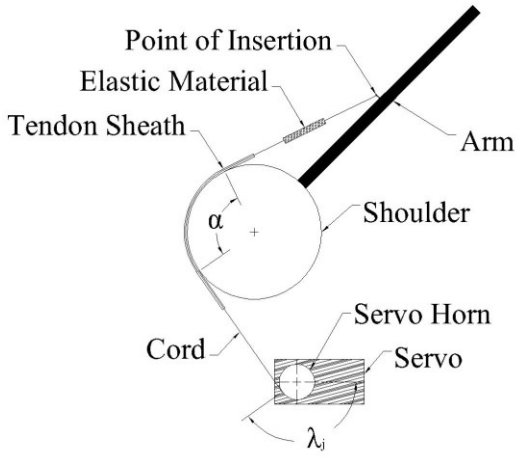

Figure 2: Our simulated "muscle-tendons" will consist of sections of elastic tubing (muscle) connected to strong cords (tendons), which are shortened by spooling on servos (see text).

Because of the in-series configuration of the components of the muscle (Figure 2) we are effectively proposing to model the muscle-tendons of the human arm as a contractile element (the servo) with an elastic element in series with it (the elastic tubing), as well as a source of friction which may be thought of as a shock-absorber or "dashpot". We believe that friction in the tendon sheaths will add effectively linearly to the elastic forces generated by the stretched tubing, so that our muscle model may be thought of as a Kelvin-Voigt viscoelastic element (cf. Winters, 1990) in series with a contractile element as shown in Figure 4.

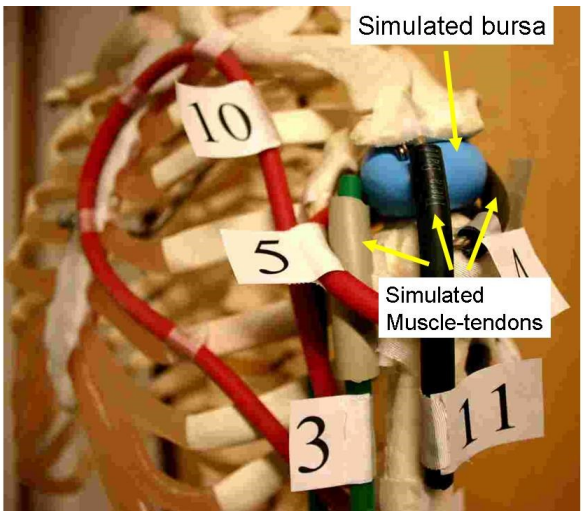

Figure 3: Photo of shoulder joint, with simulated bursa within shoulder socket. Surrounding muscle-tendons (perhaps more than in figure) will hold the bursa in place.

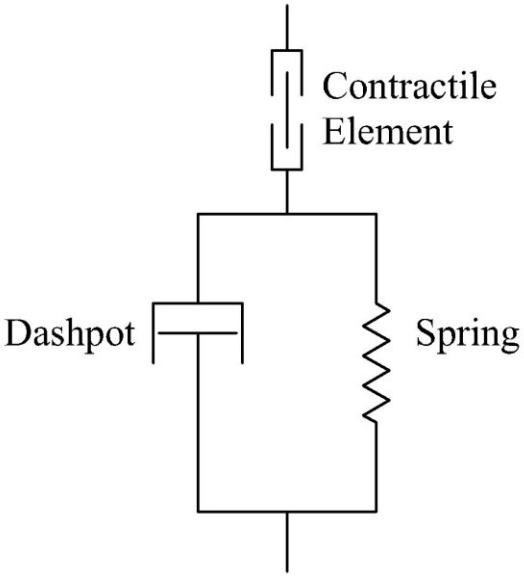

Figure 4: Our mechanical arm's muscles resemble a Kelvin-Voigt viscoelastic element in series with a contractile element.

Erin: complete this?:
now mention the list of essential muscles –(NOT including those required for pronation/supination of forearm), and refer to Figure 5 (photograph of skeleton with yarn on it). Mention that the radius and ulna of the forearm will be held securely together, eliminating the rotation of the forearm about its long axis.

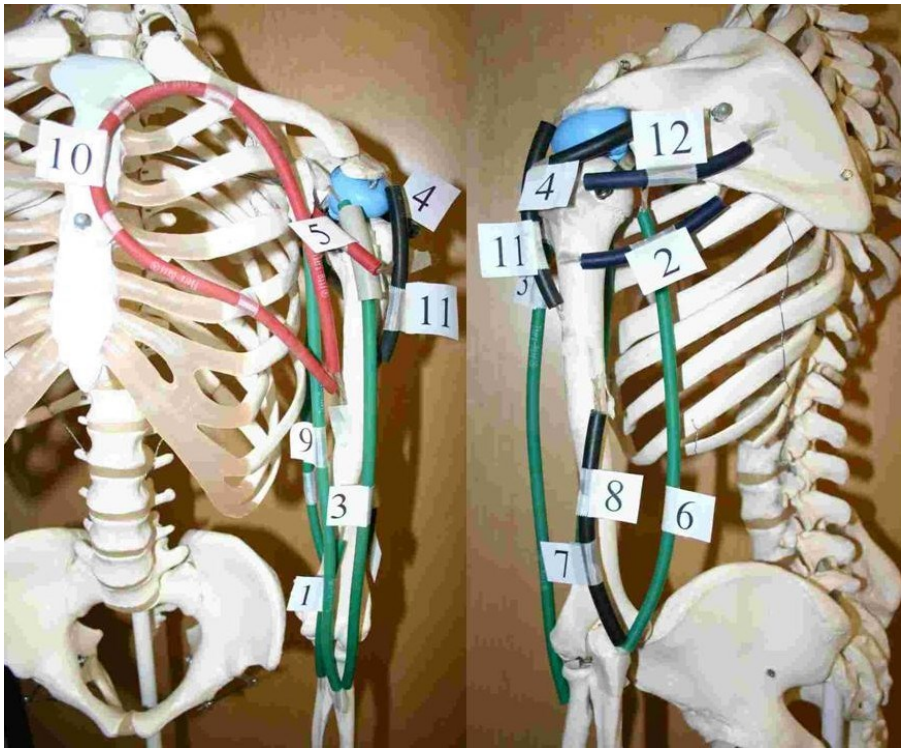

Figure 5: Model skeleton with color-coded elastic tubing showing locations of muscles. Actual muscles will have cords representing tendons, and servos attached. See text for description.

It is important to note that we do not expect our model to mimic all of the major properties of a real musculoskeletal system, because our system will be different (usually simpler) in many ways, some of which are as follows:

1) Although real muscles have been modeled as simple linear systems involving springs and shock absorbers combined with a contractile element (cf. Hill, 1938, Winters, 1990), real muscles are well known to exhibit a highly nonlinear relationship between degree of contraction and muscle force (cf. Zahalak, 1990). The Theraband© elastic tubing is also nonlinear, but obeys Hooke's Law quite well at intermediate degrees of extension where our model will probably operate. Figure 6 illustrates the relationship between restoring force and degree of stretch for a sample of the thin yellow elastic tubing (original length 19cm) shown in Figure 1, measured in our laboratory.

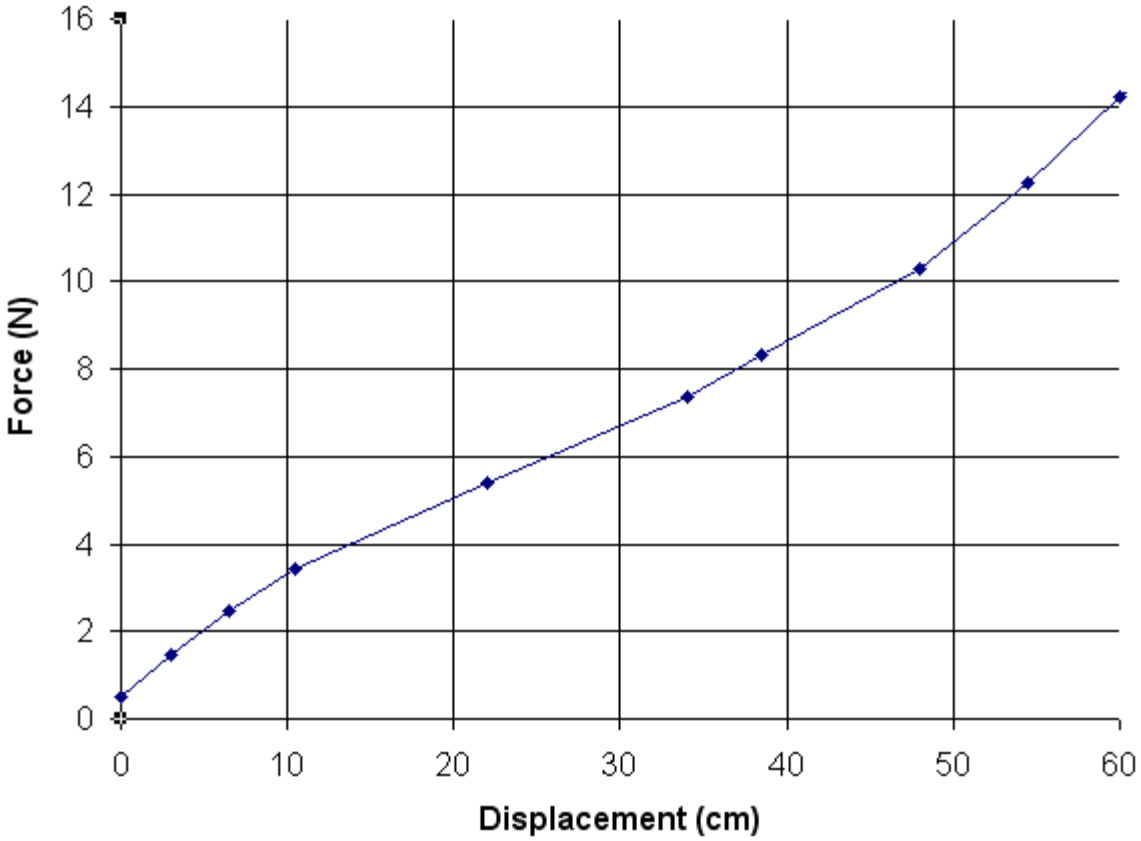

Figure 6: Force versus displacement data for sample of Theraband tubing. Original length of tube was 19cm.

2) The forces generated by actual muscles are well known to be strongly history-dependent and velocity-dependent, since muscle contractions are in reality produced by the formation of cross-bridges between actin and myosin filaments within the sarcomeres (cf. Zahalak, 1990). These cross-bridges are continuously forming and separating in a manner that depends on complex chemical reactions, and the elastic force contributed by a cross bridge changes as the filaments slide past each other during muscle motion.

3) Actual muscles are not linear in shape, and they attach to the skeletal system in a complex manner, often with a range of pennation angles along extended areas of insertion (cf. Solomon et al., 1990). Thus the degree of extension of each muscle is a complex function of limb orientation that cannot be approximated by a single linear strand.

4) Real musculoskeletal systems exhibit proprioceptive feedback – complexities arising due to the stretch reflex, and other feedback mechanisms within the central nervous system (Solomon et al.,1990). However, in our model we are only interested in the final degree of contraction of the muscles, so that this complication is unimportant for our purposes.

All of the above factors (and many others) imply that our mechanical arm will not be a realistic simulation of a true human arm. However, we view the relative simplicity of our proposed mechanical arm as a strength, rather than as a weakness, because with it we will be able to observe

complex behavior even in the absence of many of the above-mentioned complications of real systems. As a learning tool, it will allow us to see directly some of the issues necessary to modeling a real arm, while knowingly ignoring others. It will also be a fascinating application of the Lagrange's equations of motion for a complex system.

Test description: hardware

We plan to build our mechanical arm using sturdy hobby servos such as the Airt-Z servo from Hitec Corporation (Figure 7). Our initial estimates indicate that we may need as much as several hundred ounce-inches of torque (140 ounce-inches equals one Nm) for

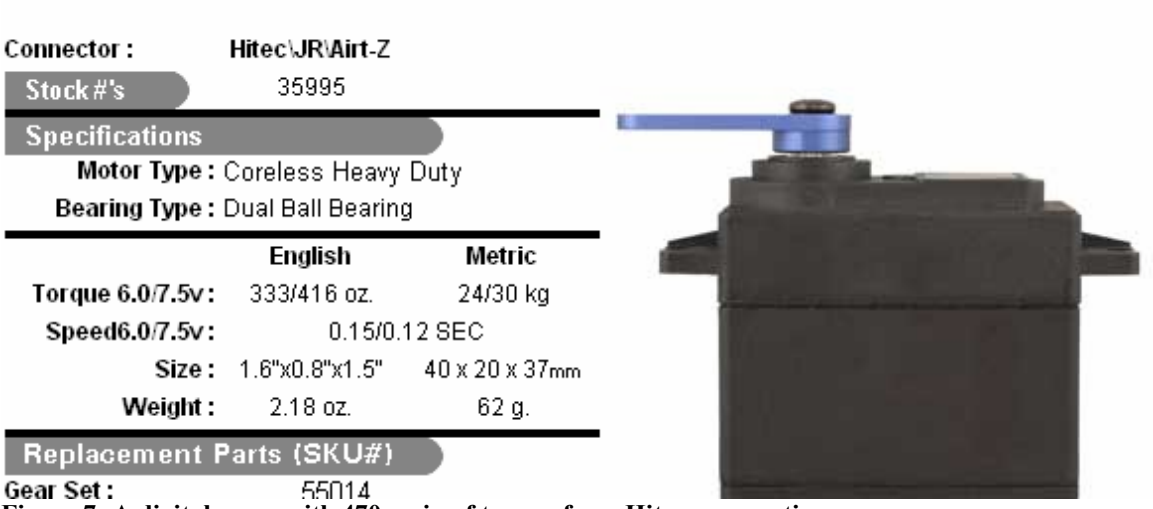

Figure 7: A digital servo with 470 oz-in of torque from Hitec corporation.

our servos to be able to hold the arm against the force of gravity, although as mentioned above, the required torques for motion in microgravity are much smaller. These strong hobby servos are therefore close to the lower limit of what we will require for our arm. If necessary, we will use additional pulleys to increase the torque supplied by the servos, by placing one or more pulleys at the points of muscle insertion and looping the muscle-tendon back to its point of origin one or more times. Furthermore, we may need to use servos capable of continuous rotation, rather than the standard angular range of between 90 and 180 degrees. Also, if necessary, we may choose to make artificial humerus, radius, and ulna bones out of light weight aluminum or wood, for example, in order to reduce gravitational torques.

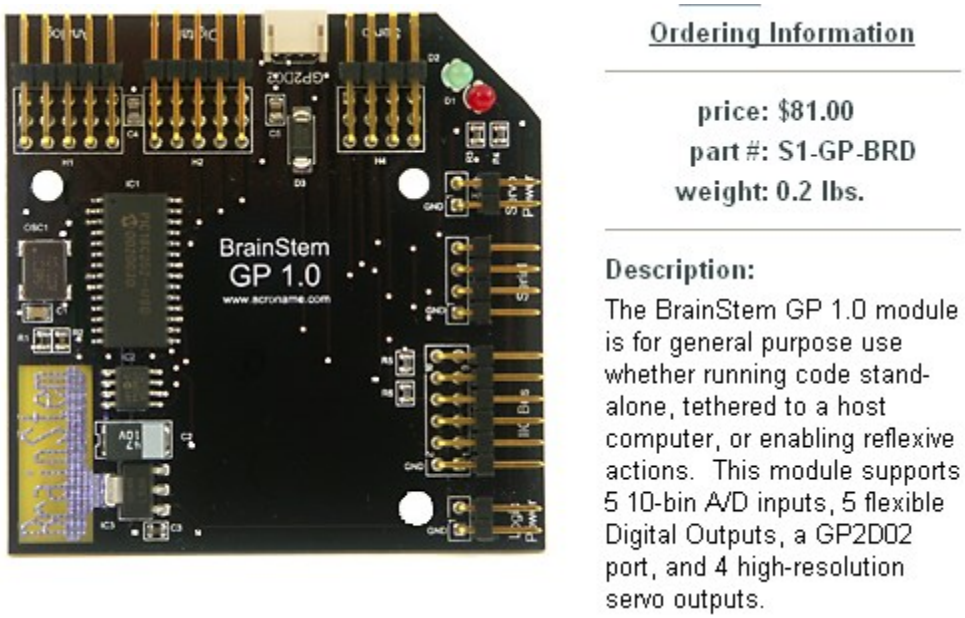

Figure 8: We plan to control our servos with three connected General Purpose Brainstem modules from Acroname Corporation.

We plan to operate the servos using three General-Purpose Brainstem modules from Acroname Incorporated (Acroname, 2005). Each of these modules (Figure 8) is capable of operating four servos, and they may be connected so that they can operate 12 servos at once – one for each of our mechanical arm's muscles. Using a USB port connection, we can thus send commands to the servos directly from a laptop computer. We already have experience at Drury University with the use of these modules from the previous experiment flown as part of the Reduced Gravity Student Flight Opportunities Program (Harris et al., 2003). We are not yet certain how we will measure the orientation of the arm while it is being manipulated by the rotation of the servos. We may use sonic motion detectors attached to the hand, or angular motion sensors of some kind, attached to the joints, that sense the true rotations of the humerus and radius-ulna of the arm at each time. Another possibility is to video the arm as it moves from at least two angles, and then to digitize the video and use Videopoint software to derive the x, y, and z positions of the end of the hand at each point in time.

Test description: Mathematical Framework

We will describe the upper part of our mechanical arm in 3-dimensional space using a standard set of Euler-angle rotations (cf. Marion and Thornton, 1995). These rotations will be initiated from an inertial coordinate system (designated by i-subscripts) with its origin at the center of the shoulder joint, and x_i, y_i, and z_i-axes directed vertically, toward the model skeleton's right, and in its forward direction, respectively, as shown in Figure 9. Thus, the upper arm's orientation is

described by the angles φ, θ_1 and ψ. The angle θ_1 describes the tilt of the upper arm away from the

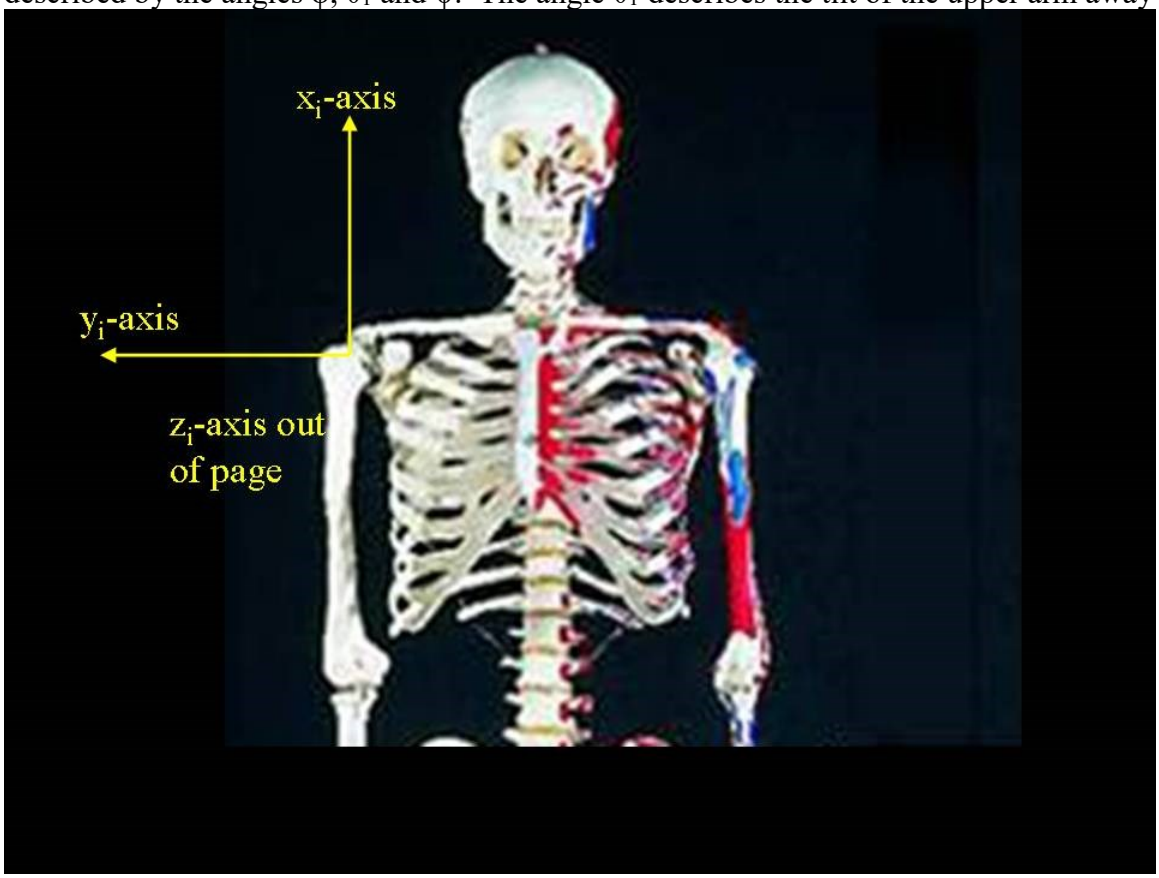

Figure 9: Inertial coordinate system for our mechanical arm mathematical framework.

skeleton's forward direction (the inertial z-axis), φ determines the direction of this tilt, and ψ describes rotation about the long axis of the upper arm. The forearm will have only one degree of freedom which can be described as a rotation about the x-axis of the upper arm's body coordinate system. This degree of freedom is described by θ_2 which is the angle of the forearm's long axis relative to that of the upper arm. Note that rotation of the forearm about its own long axis (called *pronation* and *supination,* Solomon et al., 1990) will not be included because we are primarily interested in locating the end of the hand in space, a motion to which this degree of freedom does not contribute.

In Appendix A, we describe the derivation of the equations of motion for the four degrees of freedom (φ, θ_1, ψ, and θ_2) of our proposed mechanical arm. Each of the equations may be written in Lagrange's form (Equation A24) where the left-hand and right-hand sides of the equations are expressed by equations (A25) and (A26) as given in Appendix A. All of the individual factors in the latter equations are evaluated symbolically in Appendix B. The full equations of motion are very cumbersome but can be readily integrated numerically (see below). We will be able to simplify these equations of motion considerably because the 2nd and 3rd principal moments of inertia for the forearm and upper arm are tremendously smaller than the first, since they are much longer than they are wide. We will study these equations carefully to investigate such simplifications if our proposal is accepted for flight.

The equations of motion depend on U_e , which represents the sum over all the elastic potential energies stored in each of the muscles, which we express in Appendix A as

$$U_e(\varphi,\theta_1,\psi,\theta_2,\lambda_{j=1,2,\ldots,N}) = \sum_{j=1}^{N} U_{e,j}(\varphi,\theta_1,\psi,\theta_2,\lambda_j) \tag{A16}$$

where N is the number of muscles in our mechanical arm, j is an index referring to individual muscles, and the λ_j are functions of time representing the amounts of angular rotation of the horns of each servo. Thus the λ_j describe how much each muscle-tendon is "wrapped" around its servo – the degrees of shortening of the contractile elements of the simulated muscles. Although the $U_{e,j}$ functions may in some cases be complicated algebraic expressions, they are nonetheless readily derivable in the following way: If we first express the position vectors of the points of origin and points of insertion of the muscle-tendons in the same coordinate system (whichever one makes the expression the simplest), we can then compute the lengths of their differences using the Pythagorean theorem or other simple trigonometric relationships. We can then use the fact that the Theraband tubing has an approximately linear force-length relationship (cf. Figure 6) to approximate the total stored elastic energy as a sum of simple parabolic functions:

$$U_e = \sum_{j=1}^{N} U_{e,j} = \frac{1}{2}\sum_{j=1}^{N} k_j \Delta l_j^2 \tag{1}$$

where Δl_j , which is in general a function of all four angles, is the change in length relative to resting length of the elastic part of the jth muscle-tendon and k_j are the effective spring constants for the muscle-tendons. Then the torque generated by the jth muscle-tendon, written in the equations of motion (A24, with A25 and A26), is

$$\frac{\partial U_e}{\partial q} = \sum_{j=1}^{N} \frac{\partial U_{e,j}}{\partial q} = \sum_{j=1}^{N} k_j \Delta l_j \frac{\partial \Delta l_j}{\partial q} \tag{2}$$

where q represents any of the four angular degrees of freedom (φ, θ_1, ψ, and θ_2) described above.

The equations of motion are four coupled, nonlinear differential equations with non-constant coefficients, which are tremendously difficult (if not impossible) to solve analytically, but it will be quite straightforward for us to solve them numerically (see Laboratory testing of mechanical arm section).

Laboratory testing of mechanical arm

We derived full equations of motion of the mechanical arm system in terms of the change in length of the muscles, and thus in terms of the amount of rotation of the servos controlling each muscle (See Appendix A). Armed with these equations, we can 'test' the arm by solving these equations

for chosen sets of the rotation angles λ_j as functions of time (we hereafter refer to these as *instruction sets*). Because the system is so complex, at first we will test our model by simply using the equations of motion (A24-A26) to predict the motion produced by one or more chosen instruction sets. We will integrate these equations using the Runge-Kutta method (cf. Press et al., 1997). Then we will implement these instruction sets with the arm and see if our predictions are accurate. If so, we will then begin an experimental and iterative process of solving different instruction sets for their resultant motion, with the goal of reproducing several simple motions of the arm in 3-space. Essentially, we will determine what sequence of muscle movements cause certain arm motions, such as waving good-bye or saluting, through trial and error.

The reason for this approach is practical. As already described, the equations of motion can be used to derive arm movement from a given instruction set. They can also (in principle) be used to derive the instruction set required to produce a given arm movement, and we could even introduce extra parameters to minimize (such as total energy required or total mean-squared torque change, cf. Uno et al., 1989). The latter problem, however, is extremely difficult, and is beyond the scope of this project. For our purposes, the trial-and-error approach (a *forward* approach , rather than an *inverse* approach) will suffice.

In order to numerically integrate the equations of motion, we will of course need to have reliable values of the inertia-tensor components for the upper and lower arm segments, and the relationships between the lengths of the muscle-tendons and each possible combination of the values of φ, θ_1, ψ, and θ_2 (for use in equation 2).

We will determine the inertia-tensor components in two ways: (1) we will measure masses and lengths of each segment and model the components using simple geometrical approximations (e.g. rotational inertias of long thin cylinders with "dumbbell shaped" ends for the bones) and (2) we will hang each segment by its end and measure its natural period of pendulum oscillation. Then the equation for the period of oscillation P of a physical pendulum can be used to determine the inertias:

$$P = 2\pi\sqrt{\frac{I}{mgh}} \tag{3}$$

Where m, g, I, and h are the mass, acceleration due to gravity, rotational inertia about pivot, and distance from center of mass to pivot, respectively (cf. Halliday et al., 2005).

[fill in part regarding rotational inertias about long axes measured using torsional pendulum: Adam – look up how he measured the rotational inertias of robot last time—and then write text here]

Adam: insert equation here (4)

We will determine the relationships between the lengths of the muscle-tendons for each possible combination of the values of φ, θ_1, ψ, and θ_2 both (1) algebraically (see previous section), and (2)

by inserting digital force sensors from our General Physics laboratory equipment in-line with the muscle-tendons, and then moving the arm through a wide range of angular positions, and recording the stretching force for each muscle at each angular orientation. Using Hooke's law, we can then transform these forces into derived values of the amount of stretch of each muscle. We will use the data collected from (2) to find the least-squares best fits to the algebraic formulae derived in (1).

Experiment in zero gravity

Make longer?

The equations of motion we find for the mechanical arm (A24-A26, B18, B19) depend on the acceleration due to gravity, *g*. The goal of the experiment is to take these instruction sets and have the mechanical arm carry out the same sequence of muscle contractions as it would on the surface of the earth, and measure the resulting arm movement. We can predict the movement by solving the equations of motion a second time with $g = 0$, but to test our predictions we will need to carry out the experiment in a microgravity environment.

[One interesting and simple question is how different the motions would be, given the exact same servo-rotation command sequence.]

[CAN DELETE NOW?: Nathan will write:

Describe how the equations of Appendix A simplify when g is set to zero.

We will predict motions in microgravity, given pre-planned sets of servo motions, and see how well they compare.

One interesting and simple question is how different the motions would be, given the exact same servo-rotation command sequence.

A much more difficult question is how to make the hand execute a prescribed trajectory -- the "inverse" problem. We will think about this question, but we will probably need to confine ourselves to the "forward" problem of predicting motions resulting from prescribed servo rotations.]

Appendix A: Equations of motion for mechanical arm

In order to obtain the equations of motion for our mechanical arm, we will apply Hamilton's Principle to the Lagrangian for the system (cf. Marion and Thornton, 1995). Accordingly, we must first obtain expressions for the kinetic and potential energies for all parts of the arm system, written in terms of the angular degrees of freedom (φ, θ_1, ψ, and θ_2) as described in the *Test description: mathematical framework* section of this proposal. Following the standard development for Euler angle rotations, we may transform vectors from inertial space (x_i, y_i, z_i –see Figure 9) to the standard body coordinate system (which we denote by x_t, y_t, z_t) of a rigid body with its end fixed,

by performing rotations of φ, θ_1, and ψ about the z_i , x', and z''-axes, successively, where the primed and double-primed variables represent Cartesian coordinates of the intermediate coordinate systems in the succession of rotational transformations. These rotational transformations are effected by the rotation matrices

$$\Lambda_{\varphi} = \begin{bmatrix} \cos\varphi & \sin\varphi & 0 \\ -\sin\varphi & \cos\varphi & 0 \\ 0 & 0 & 1 \end{bmatrix} \tag{A1}$$

$$\Lambda_{\theta_1} = \begin{bmatrix} 1 & 0 & 0 \\ 0 & \cos\theta_1 & \sin\theta_1 \\ 0 & -\sin\theta_1 & \cos\theta_1 \end{bmatrix} \tag{A2}$$

$$\Lambda_{\psi} = \begin{bmatrix} \cos\psi & \sin\psi & 0 \\ -\sin\psi & \cos\psi & 0 \\ 0 & 0 & 1 \end{bmatrix} \tag{A3}$$

The body coordinate system thus reached (x_t, y_t, z_t) is, however, not convenient should we want to consider the simpler problem of motion in the horizontal plane, because most research by others in the field of human arm mechanics uses an upper arm coordinate system where the upper arm is directed along the x-axis of the its body coordinate system, and the with the z-axis is vertical, as shown in Figure 10 (cf. Scott, 1999, Uno et al., 1989). For this reason we add one additional

rotational transformation:

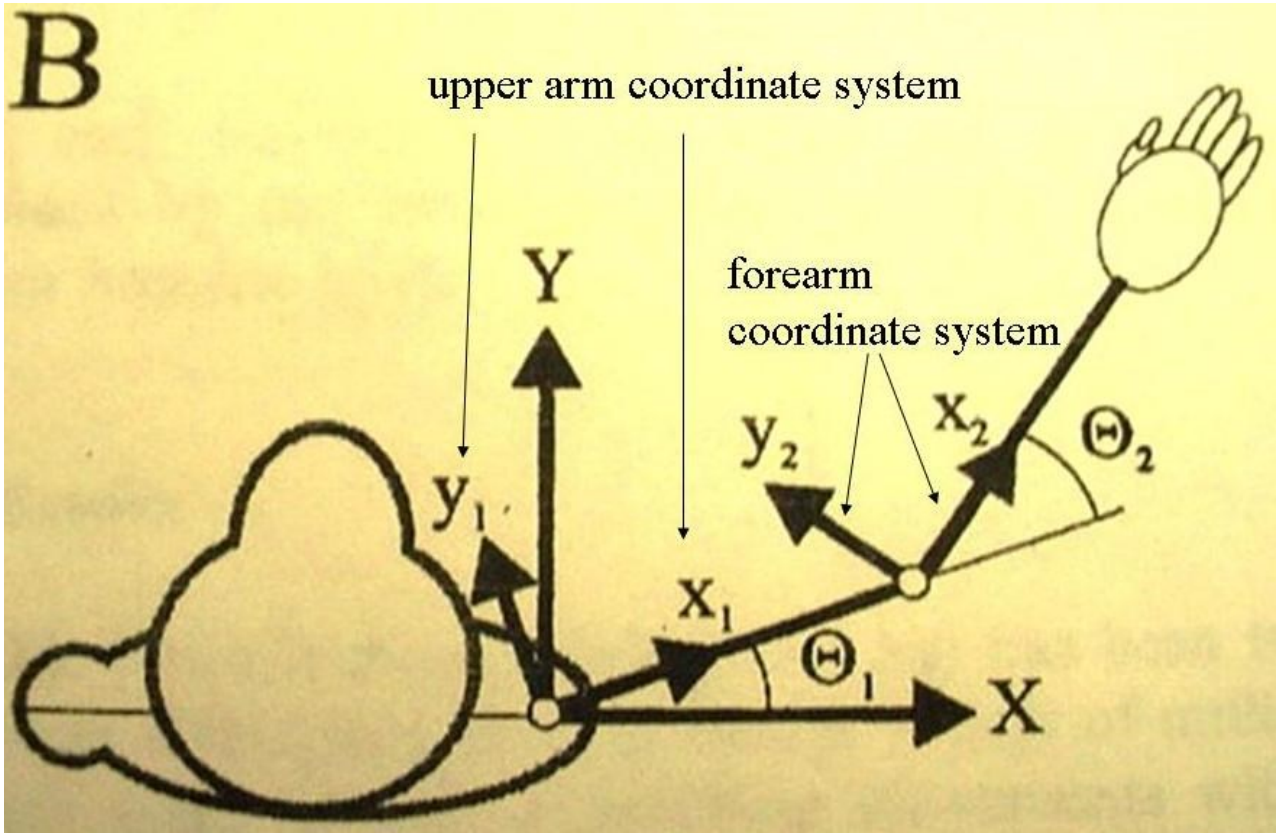

Figure 10: Standard planar coordinate systems for upper arm and forearm (modified from Scott, 1999).

we interchange the x_t and z_t-axes, and invert the y_t-axis (to keep the coordinate system right-handed). This transformation is effected by the matrix

$$\Lambda_{tu} = \begin{bmatrix} 0 & 0 & 1 \\ 0 & -1 & 0 \\ 1 & 0 & 0 \end{bmatrix} \tag{A4}$$

By adding this transformation, our equations of motion will reduce to the well-documented equations for planar arm motion, if we set $\varphi=0$ or $\varphi=\pi$.

Additionally, locations in the upper arm body-coordinate system are transformed to that of the forearm by a translation of the length l_1 of the upper arm along the z_u-axis,

$$\vec{l}_{1u} = \begin{bmatrix} l_1 \\ 0 \\ 0 \end{bmatrix} \tag{A5}$$

and a rotation about the x_u-axis by the angle θ_2, i.e. using the rotation matrix:

$$\Lambda_{\theta_2} = \begin{bmatrix} \cos\theta_2 & \sin\theta_2 & 0 \\ -\sin\theta_2 & \cos\theta_2 & 0 \\ 0 & 0 & 1 \end{bmatrix} \tag{A6}$$

Kinetic energy of upper arm:

If we choose the body coordinate system of the upper arm to coincide with the upper arm's principal axes of inertia, the kinetic energy of the upper arm is simply

$$T_u = \frac{1}{2}\left(I_{1u}\omega_{1u,u}^2 + I_{2u}\omega_{2u,u}^2 + I_{3u}\omega_{3u,u}^2\right) \tag{A7}$$

where

$$\vec{\omega}_{u,u} \equiv \begin{bmatrix} \omega_{1u,u} \\ \omega_{2u,u} \\ \omega_{3u,u} \end{bmatrix} = \begin{bmatrix} \dot{\varphi}\cos\theta_1 + \dot{\psi} \\ -\dot{\varphi}\cos\psi\sin\theta_1 + \dot{\theta}_1\sin\psi \\ \dot{\varphi}\sin\psi\sin\theta_1 + \dot{\theta}_1\cos\psi \end{bmatrix} \tag{A8}$$

is the angular velocity vector of the upper arm, expressed in the body-coordinate system of the upper arm, and the I_{iu} are computed about the pivot (the origin of the inertial coordinate system shown in Figure 9).

Kinetic energy of the forearm:

The total kinetic energy of the forearm can be written as the sum of the translational kinetic energy of a point-mass M_f (equal to forearm mass) located at the forearm's center of mass, and the rotational kinetic energy of the forearm about its center of mass, as follows:

$$T_f = \frac{1}{2}M_f v_{f,cm}^2 + \frac{1}{2}\left(I_{1f}\omega_{1f,f}^2 + I_{2f}\omega_{2f,f}^2 + I_{3f}\omega_{3f,f}^2\right) \tag{A9}$$

where

$$\vec{\omega}_{f,f} \equiv \begin{bmatrix} \omega_{1f,f} \\ \omega_{2f,f} \\ \omega_{3f,f} \end{bmatrix} = \begin{bmatrix} \dot{\varphi}(\cos\theta_1 \cos\theta_2 - \cos\psi \sin\theta_1 \sin\theta_2) + \dot{\theta}_1 \sin\psi \sin\theta_2 + \dot{\psi}\cos\theta_2 \\ \dot{\varphi}(-\cos\theta_1 \sin\theta_2 - \cos\psi \sin\theta_1 \cos\theta_2) + \dot{\theta}_1 \sin\psi \cos\theta_2 - \dot{\psi}\sin\theta_2 \\ \dot{\varphi}\sin\psi \sin\theta_1 + \dot{\theta}_1 \cos\psi + \dot{\theta}_2 \end{bmatrix} \tag{A10}$$

is the angular velocity of the forearm, measured in the body coordinate system of the forearm, and the I_{if} are the principal moments of inertia of the forearm, calculated about the center of mass of the forearm. Also,

$$\vec{v}_{f,cm} = \vec{V}_{f,e} + \vec{\omega}_{f,f} \times \vec{R}_{f,cm} \tag{A11}$$

is the velocity of the center of mass of the forearm in the forearm's body coordinate system, where

$$\vec{V}_{f,e} = \Lambda_{\theta_2}(\vec{\omega}_{u,u} \times \vec{l}_{1,e}) = l_1 \begin{bmatrix} \omega_{3u,u} \sin\theta_2 \\ \omega_{3u,u} \cos\theta_2 \\ -\omega_{2u,u} \end{bmatrix} \tag{A12}$$

is the velocity of the elbow measured in the body coordinate system of the forearm, and

$$\vec{R}_{f,cm} = \begin{bmatrix} R_{fcm} \\ 0 \\ 0 \end{bmatrix} \tag{A13}$$

is the position of the forearm's center of mass, measured in the body coordinate system of the forearm. Combining equations (A7), (A9) and (A11) through (A13) we can finally express the total kinetic energy of the mechanical arm as

$$T_{total} = \frac{1}{2}\left(I'_{1u}\omega^2_{1u,u} + I'_{2u}\omega^2_{2u,u} + I'_{3u}\omega^2_{3u,u}\right) + \frac{1}{2}\left(I'_{1f}\omega^2_{1f,f} + I'_{2f}\omega^2_{2f,f} + I'_{3f}\omega^2_{3f,f}\right) + c(\omega_{2u}\omega_{2f} + \omega_{3u}\omega_{3f}) \tag{A14}$$

where

$$
\begin{aligned}
I'_{1u} &\equiv I_{1u} \\
I'_{2u} &\equiv I_{2u} + \frac{M_f l_1^2}{2} \\
I'_{3u} &\equiv I_{3u} + \frac{M_f l_1^2}{2} \\
I'_{1f} &\equiv I_{1f} \\
I'_{2f} &\equiv I_{2f} + \frac{M\ R_{cm}^2}{2} \\
I'_{3f} &\equiv I_{3f} + \frac{M\ R_{cm}^2}{2}
\end{aligned}
\tag{A15}
$$

Elastic potential energy of the mechanical arm:

As mentioned in the *Test description: mathematical framework* section, the total elastic potential energy U_e represents the sum over all the elastic potential energies stored in each of the muscles, which we can express as

$$
U_e(\varphi, \theta_1, \psi, \theta_2, \lambda_{j=1,2,\ldots,N}) = \sum_{j=1}^{N} U_{e,j}(\varphi, \theta_1, \psi, \theta_2, \lambda_j) \tag{A16}
$$

where N is the number of muscles in our mechanical arm, j is an index referring to individual muscles, and the λ_j are functions of time representing the amounts of angular rotation of the horns of each servo (see Figure 2 for a simple example). Thus the λ_j describe how much each muscle-tendon is "wrapped" around its servo – the degrees of shortening of the contractile elements of the simulated muscles. In the above-mentioned section of this proposal, we explain how we plan to determine the $U_{e,j}$ functions in the laboratory.

Gravitational potential energy of the upper arm:

The gravitational potential energy of a rigid body is equivalent to that of an equal point mass located at the center of mass of the object (cf. Marion and Thornton, 1995). Because the body coordinate systems for the upper arm and the forearm will be principal axes, their centers of mass will be directed along their respective x-axes, at distances defined to be R_{ucm} and R_{fcm}, respectively. Equation A11 gives the position of the forearm center of mass in the forearm's body coordinate system. Similarly, the position of the upper arm's center of mass in the body coordinate system of the upper arm is

$$\vec{R}_{ucm} = \begin{bmatrix} R_{ucm} \\ 0 \\ 0 \end{bmatrix} \tag{A17}$$

We can easily express this vector in the inertial coordinate system by performing the matrix rotations in reverse:

$$\vec{R}_{ucm,i} = \Lambda^t_{\varphi}\Lambda^t_{\theta_1}\Lambda^t_{\psi}\Lambda^t_{tu}\vec{R}_{ucm} = \begin{bmatrix} R_{ucm}\sin\theta_1\sin\varphi \\ -R_{ucm}\sin\theta_1\cos\varphi \\ R_{ucm}\cos\theta_1 \end{bmatrix} \tag{A18}$$

Now, since the vertical coordinate in the inertial coordinate system is x_i, the gravitational potential energy of the upper arm U_{gu} is simply the product of its mass M_u with the acceleration due to gravity g, and the x_i-component of its center of mass:

$$U_{gu} = M_u g R_{ucm}\sin\theta_1\sin\varphi \tag{A19}$$

Gravitational potential energy of the forearm:

The gravitational potential energy of the forearm is obtained in the identical manner to that of the upper arm, except that the center of mass of the forearm, measured in the coordinate system of the upper arm, is

$$\vec{R}_{fcm,u} = \vec{l}_{1,u} + \Lambda^t_{\theta_2}\vec{R}_{fcm,f} = \begin{bmatrix} l_1 + R_{fcm}\cos\theta_2 \\ R_{fcm}\sin\theta_2 \\ 0 \end{bmatrix} \tag{A20}$$

Then the same inverse-rotations that we used for the upper arm are used to express the position of the forearm's center of mass in the inertial coordinate system, yielding:

$$\vec{R}_{fcm,i} = l_1\begin{bmatrix} \sin\theta_1\sin\varphi \\ -\sin\theta_1\cos\varphi \\ \cos\theta_1 \end{bmatrix} + R_{fcm}\begin{bmatrix} \cos\varphi\sin\psi\sin\theta_2 + \sin\varphi(\cos\psi\cos\theta_1\sin\theta_2 + \sin\theta_1\cos\theta_2) \\ \sin\varphi\sin\psi\sin\theta_2 - \cos\varphi(\cos\psi\cos\theta_1\sin\theta_2 + \sin\theta_1\cos\theta_2) \\ -\cos\psi\sin\theta_1\sin\theta_2 + \cos\theta_1\cos\theta_2 \end{bmatrix} \tag{A21}$$

The gravitational potential energy of the forearm, U_{gf}, is the product of its mass M_f with the acceleration due to gravity g, and the x_i-component of its center of mass:

$$U_{gf} = M_f g\{l_1 \sin\theta_1 \sin\varphi + R_{fcm}[\cos\varphi \sin\psi \sin\theta_2 + \sin\varphi(\cos\psi \cos\theta_1 \sin\theta_2 + \sin\theta_1 \cos\theta_2)]\} \textbf{(A22)}$$

The Lagrangian for the mechanical arm:

The Lagrangian is the difference between the total kinetic energy and the total potential energy of the mechanical arm system with all of its muscles:

$$L \equiv T_{total} - (U_e + U_{gu} + U_{gf}) \tag{A23}$$

Where T_{total}, U_e, U_{gu} and U_{gf} are given by equations *, *, *, and *. Note that all four of these quantities are functions of the angles φ, θ_1, ψ, and θ_2. In addition, T_{total} is also a function of the time derivatives of the angles, and U_e is a function of the servo rotation angles λ_j, which will be prescribed functions of time. Thus, Lagrange's equations of motion still apply, except that the energy of the system is not constant in time. This is obviously true because the servos will continuously add energy (and subtract it) from the system as the arm moves.

The equations of motion:

To obtain the equation of motion for each of the angles, designated generically by q_i, we simply apply Lagrange's equations of motion (cf. Marion and Thornton, 1995):

$$\frac{d}{dt}\left(\frac{\partial L}{\partial \dot{q}}\right) = \frac{\partial L}{\partial q} \tag{A24}$$

for each coordinate.

Using equations (A7),(A9),(A16),(A19) we can thus write the left-hand side of equation (A24) in the form

$$\frac{d}{dt}\left(\frac{\partial L}{\partial \dot{q}}\right) = \sum_{i=1}^{3} I'_{iu}\left[\dot{\omega}_{iu}\frac{\partial \omega_{iu}}{\partial \dot{q}} + \omega_{iu}\frac{d}{dt}\left(\frac{\partial \omega_{iu}}{\partial \dot{q}}\right)\right] + \sum_{i=1}^{3} I'_{if}\left[\dot{\omega}_{if}\frac{\partial \omega_{if}}{\partial \dot{q}} + \omega_{if}\frac{d}{dt}\left(\frac{\partial \omega_{if}}{\partial \dot{q}}\right)\right] +$$
$$c\sum_{i=2}^{3}\left[\frac{d\omega_{iu}}{dt}\frac{\partial \omega_{if}}{\partial \dot{q}} + \omega_{iu}\frac{d}{dt}\left(\frac{\partial \omega_{if}}{\partial \dot{q}}\right)\right] + c\sum_{i=2}^{3}\left[\frac{d\omega_{if}}{dt}\frac{\partial \omega_{iu}}{\partial \dot{q}} + \omega_{if}\frac{d}{dt}\left(\frac{\partial \omega_{iu}}{\partial \dot{q}}\right)\right] \tag{A25}$$

and we can write the right-hand side of equation (A24) in the form

$$\frac{\partial L}{\partial q} = \sum_{i=1}^{3} I'_{iu}\omega_{iu}\frac{\partial \omega_{iu}}{\partial q} + \sum_{i=1}^{3} I'_{if}\omega_{if}\frac{\partial \omega_{if}}{\partial q} + c\sum_{i=2}^{3}\left[\omega_{iu}\frac{\partial \omega_{if}}{\partial q} + \omega_{if}\frac{\partial \omega_{iu}}{\partial q}\right] - \left[\frac{\partial U_{gu}}{\partial q} + \frac{\partial U_{gf}}{\partial q} + \frac{\partial U_{e}}{\partial q}\right] \quad \text{(A26)}$$

Because including all of the various required derivatives of the angular velocity components in the above expressions would be extremely cumbersome, we have included these derivatives separately, in Appendix B. However, note that each derivative term above is simply a function of the four angles and their first and/or second time derivatives. Therefore, although the equations are complex in form, there is nothing intrinsically difficult in solving them numerically. As described in the *Laboratory testing of mechanical arm* and the *Experiment in zero gravity* sections of this proposal, we will use a standard Runge-Kutta numerical integration scheme to solve for the motion of the arm for various planned motions of the servos which control the muscles.

Appendix B: Derivatives of the angular velocities and gravitational potential energies

The equations of motion (A24 combined with A25, A26) contain the following derivatives which are expressed here in their full form:

$$\begin{aligned}
\frac{d\omega_{1u}}{dt} &= \ddot{\varphi}\cos\theta_1 + \ddot{\psi} - \dot{\varphi}\dot{\theta}_1\sin\theta_1 \\
\frac{d\omega_{2u}}{dt} &= -\ddot{\varphi}\sin\theta_1\cos\psi + \ddot{\theta}_1\sin\psi - \dot{\varphi}\dot{\theta}_1\cos\theta_1\cos\psi + \dot{\varphi}\dot{\psi}\sin\theta_1\sin\psi + \dot{\theta}_1\dot{\psi}\cos\psi \\
\frac{d\omega_{3u}}{dt} &= -\ddot{\varphi}\sin\theta_1\sin\psi + \ddot{\theta}_1\cos\psi + \dot{\varphi}\dot{\theta}_1\cos\theta_1\sin\psi + \dot{\varphi}\dot{\psi}\sin\theta_1\cos\psi - \dot{\theta}_1\dot{\psi}\sin\psi
\end{aligned} \quad \text{(B1)}$$

$$\frac{d\omega_{1f}}{dt} = \ddot{\varphi}\left[\cos\theta_1\cos\theta_2 - \sin\theta_1\sin\theta_2\cos\psi\right] + \ddot{\theta}_1\sin\psi\sin\theta_2 + \ddot{\psi}\cos\theta_2 - \dot{\varphi}\dot{\theta}_1\left(\sin\theta_1\cos\theta_2 + \cos\theta_1\sin\theta_2\cos\psi\right) + \dot{\varphi}\dot{\psi}\sin\theta_1\sin\theta_2\sin\psi$$
$$- \dot{\varphi}\dot{\theta}_2\left[\cos\theta_1\sin\theta_2 + \sin\theta_1\cos\theta_2\cos\psi\right] + \dot{\theta}_1\dot{\psi}\cos\psi\sin\theta_2 + \dot{\theta}_1\dot{\theta}_2\sin\psi\cos\theta_2 - \dot{\psi}\dot{\theta}_2\sin\theta_2$$

$$\frac{d\omega_{2f}}{dt} = \ddot{\varphi}\left[-\cos\theta_1\sin\theta_2 - \sin\theta_1\cos\theta_2\cos\psi\right] + \ddot{\theta}_1\sin\psi\cos\theta_2 - \ddot{\psi}\sin\theta_2 - \dot{\varphi}\dot{\theta}_1\left(\sin\theta_1\sin\theta_2 - \cos\theta_1\cos\theta_2\cos\psi\right) + \dot{\varphi}\dot{\psi}\sin\theta_1\cos\theta_2\sin\psi$$
$$+ \dot{\varphi}\dot{\theta}_2\left[-\cos\theta_1\cos\theta_2 + \sin\theta_1\sin\theta_2\cos\psi\right] + \dot{\theta}_1\dot{\psi}\cos\psi\cos\theta_2 - \dot{\theta}_1\dot{\theta}_2\sin\psi\sin\theta_2 - \dot{\psi}\dot{\theta}_2\cos\theta_2$$

$$\frac{d\omega_{3f}}{dt} = \ddot{\varphi}\sin\theta_1\sin\psi + \ddot{\theta}_1\cos\psi + \ddot{\theta} + \dot{\varphi}\dot{\theta}_1\cos\theta_1\sin\psi + \dot{\varphi}\dot{\psi}\sin\theta_1\cos\psi - \dot{\theta}_1\dot{\psi}\sin\psi \tag{B2}$$

$$\frac{\partial\omega_{1u}}{\partial\dot{\varphi}} = \cos\theta_1$$
$$\frac{\partial\omega_{1u}}{\partial\dot{\theta}_1} = 0$$
$$\frac{\partial\omega_{1u}}{\partial\dot{\psi}} = 1 \tag{B3}$$
$$\frac{\partial\omega_{1u}}{\partial\dot{\theta}_2} = 0$$

$$\frac{\partial\omega_{2u}}{\partial\dot{\varphi}} = -\cos\psi\sin\theta_1$$
$$\frac{\partial\omega_{2u}}{\partial\dot{\theta}_1} = \sin\psi$$
$$\frac{\partial\omega_{2u}}{\partial\dot{\psi}} = 0 \tag{B4}$$
$$\frac{\partial\omega_{2u}}{\partial\dot{\theta}_2} = 0$$

$$\frac{\partial \omega_{3u}}{\partial \dot{\varphi}} = \sin\psi \sin\theta_1$$
$$\frac{\partial \omega_{3u}}{\partial \dot{\theta}_1} = \cos\psi$$
$$\frac{\partial \omega_{3u}}{\partial \dot{\psi}} = 0 \qquad \text{(B5)}$$
$$\frac{\partial \omega_{3u}}{\partial \dot{\theta}_2} = 0$$

$$\frac{\partial \omega_{1f}}{\partial \dot{\varphi}} = \cos\theta_1 \cos\theta_2 - \cos\psi \sin\theta_1 \sin\theta_2$$
$$\frac{\partial \omega_{1f}}{\partial \dot{\theta}_1} = \sin\psi \sin\theta_2$$
$$\frac{\partial \omega_{1f}}{\partial \dot{\psi}} = \cos\theta_2 \qquad \text{(B6)}$$
$$\frac{\partial \omega_{1f}}{\partial \dot{\theta}_2} = 0$$

$$\frac{\partial \omega_{2f}}{\partial \dot{\varphi}} = \left(-\cos\theta_1 \sin\theta_2 - \cos\psi \sin\theta_1 \cos\theta_2\right)$$
$$\frac{\partial \omega_{2f}}{\partial \dot{\theta}_1} = \sin\psi \cos\theta_2$$
$$\frac{\partial \omega_{2f}}{\partial \dot{\psi}} = -\sin\theta_2 \qquad \text{(B7)}$$
$$\frac{\partial \omega_{2f}}{\partial \dot{\theta}_2} = 0$$

$$\frac{\partial \omega_{3f}}{\partial \dot{\varphi}} = \sin\psi \sin\theta_1$$
$$\frac{\partial \omega_{3f}}{\partial \dot{\theta}_1} = \cos\psi$$
$$\frac{\partial \omega_{3f}}{\partial \dot{\psi}} = 0 \qquad \text{(B8)}$$
$$\frac{\partial \omega_{3f}}{\partial \dot{\theta}_2} = 1$$

$$\frac{d}{dt}\left(\frac{\partial \omega_{1u}}{\partial \dot{\varphi}}\right) = -\dot{\theta}\ \sin\theta_1$$
$$\frac{d}{dt}\left(\frac{\partial \omega_{1u}}{\partial \dot{\theta}_1}\right) = 0$$
$$\frac{d}{dt}\left(\frac{\partial \omega_{1u}}{\partial \dot{\psi}}\right) = 0 \qquad \text{(B9)}$$
$$\frac{d}{dt}\left(\frac{\partial \omega_{1u}}{\partial \dot{\theta}_2}\right) = 0$$

$$\frac{d}{dt}\left(\frac{\partial \omega_{2u}}{\partial \dot{\varphi}}\right) = -\dot{\theta}_1 \cos\theta_1 \cos\psi + \dot{\psi} \sin\theta_1 \sin\psi$$
$$\frac{d}{dt}\left(\frac{\partial \omega_{2u}}{\partial \dot{\theta}_1}\right) = \dot{\psi} \cos\psi$$
$$\frac{d}{dt}\left(\frac{\partial \omega_{2u}}{\partial \dot{\psi}}\right) = 0 \qquad \text{(B10)}$$
$$\frac{d}{dt}\left(\frac{\partial \omega_{2u}}{\partial \dot{\theta}_2}\right) = 0$$

$$\frac{d}{dt}\left(\frac{\partial \omega_{3u}}{\partial \dot{\varphi}}\right) = \dot{\theta}_1 \cos\theta_1 \sin\psi + \dot{\psi} \sin\theta_1 \cos\psi$$
$$\frac{d}{dt}\left(\frac{\partial \omega_{3u}}{\partial \dot{\theta}_1}\right) = -\dot{\psi} \sin\psi$$
$$\frac{d}{dt}\left(\frac{\partial \omega_{3u}}{\partial \dot{\psi}}\right) = 0 \qquad \text{(B11)}$$
$$\frac{d}{dt}\left(\frac{\partial \omega_{3u}}{\partial \dot{\theta}_2}\right) = 0$$

$$\frac{d}{dt}\left(\frac{\partial \omega_{1f}}{\partial \dot{\varphi}}\right) = -\dot{\theta}_1\left(\sin\theta_1\cos\theta_2 + \cos\theta_1\sin\theta_2\cos\psi\right) - \dot{\theta}_2\left(\cos\theta_1\sin\theta_2 + \sin\theta_1\cos\theta_2\cos\psi\right) + \dot{\psi}\sin\theta_1\sin\theta_2\sin\psi$$

$$\frac{d}{dt}\left(\frac{\partial \omega_{1f}}{\partial \dot{\theta}_1}\right) = \dot{\theta}_2\sin\psi\cos\theta_2 + \dot{\psi}\cos\psi\sin\theta_2$$

$$\frac{d}{dt}\left(\frac{\partial \omega_{1f}}{\partial \dot{\psi}}\right) = -\dot{\theta}_2\sin\theta_2$$

$$\frac{d}{dt}\left(\frac{\partial \omega_{1f}}{\partial \dot{\theta}_2}\right) = 0$$

(B12)

$$\frac{d}{dt}\left(\frac{\partial \omega_{2f}}{\partial \dot{\varphi}}\right) = \dot{\theta}_1\left(\sin\theta_1\sin\theta_2 - \cos\theta_1\cos\theta_2\cos\psi\right) - \dot{\theta}_2\left(\cos\theta_1\cos\theta_2 - \sin\theta_1\sin\theta_2\cos\psi\right) + \dot{\psi}\sin\theta_1\cos\theta_2\sin\psi$$

$$\frac{d}{dt}\left(\frac{\partial \omega_{2f}}{\partial \dot{\theta}_1}\right) = -\dot{\theta}_2\sin\psi\sin\theta_2 + \dot{\psi}\cos\psi\cos\theta_2$$

$$\frac{d}{dt}\left(\frac{\partial \omega_{2f}}{\partial \dot{\psi}}\right) = -\dot{\theta}_2\cos\theta_2$$

$$\frac{d}{dt}\left(\frac{\partial \omega_{2f}}{\partial \dot{\theta}_2}\right) = 0$$

(B13)

$$\frac{d}{dt}\left(\frac{\partial \omega_{3f}}{\partial \dot{\varphi}}\right) = \dot{\theta}_1\cos\theta_1\sin\psi + \dot{\psi}\sin\theta_1\cos\psi$$

$$\frac{d}{dt}\left(\frac{\partial \omega_{3f}}{\partial \dot{\theta}_1}\right) = -\dot{\psi}\sin\psi$$

$$\frac{d}{dt}\left(\frac{\partial \omega_{3f}}{\partial \dot{\psi}}\right) = 0$$

$$\frac{d}{dt}\left(\frac{\partial \omega_{3f}}{\partial \dot{\theta}_2}\right) = 0$$

(B14)

$$\frac{\partial \omega_{1u}}{\partial \varphi} = 0$$
$$\frac{\partial \omega_{1u}}{\partial \theta_1} = -\dot{\varphi} \sin \theta_1$$
$$\frac{\partial \omega_{1u}}{\partial \psi} = 0$$
$$\frac{\partial \omega_{1u}}{\partial \theta_2} = 0 \tag{B15}$$

$$\frac{\partial \omega_{2u}}{\partial \varphi} = 0$$
$$\frac{\partial \omega_{2u}}{\partial \theta_1} = -\dot{\varphi} \cos \theta_1 \cos \psi$$
$$\frac{\partial \omega_{2u}}{\partial \psi} = \dot{\varphi} \sin \theta_1 \sin \psi + \dot{\theta}_1 \cos \psi$$
$$\frac{\partial \omega_{2u}}{\partial \theta_2} = 0 \tag{B16}$$

$$\frac{\partial \omega_{3u}}{\partial \varphi} = 0$$
$$\frac{\partial \omega_{3u}}{\partial \theta_1} = \dot{\varphi} \cos \theta_1 \sin \psi$$
$$\frac{\partial \omega_{3u}}{\partial \psi} = \dot{\varphi} \sin \theta_1 \cos \psi - \dot{\theta}_1 \sin \psi$$
$$\frac{\partial \omega_{3u}}{\partial \theta_2} = 0 \tag{B17}$$

$$\begin{aligned}
\frac{\partial U_{gu}}{\partial \varphi} &= M_u g R_{ucm} \cos\varphi \sin\theta_1 \\
\frac{\partial U_{gu}}{\partial \theta_1} &= M_u g R_{ucm} \sin\varphi \cos\theta_1 \\
\frac{\partial U_{gu}}{\partial \psi} &= 0 \\
\frac{\partial U_{gu}}{\partial \theta_2} &= 0
\end{aligned} \tag{B18}$$

$$\begin{aligned}
\frac{\partial U_{gf}}{\partial \varphi} &= M_f g \left\{ l_1 \sin\theta_1 \cos\varphi + R_{fcm} \left[-\sin\varphi \sin\theta_2 \sin\psi + \cos\varphi (\cos\theta_1 \sin\theta_2 \cos\psi + \sin\theta_1 \cos\theta_2) \right] \right\} \\
\frac{\partial U_{gf}}{\partial \theta_1} &= M_f g \left\{ l_1 \cos\theta_1 \sin\varphi + R_{fcm} \sin\varphi (-\sin\theta_1 \sin\theta_2 \cos\psi + \cos\theta_1 \cos\theta_2) \right\} \\
\frac{\partial U_{gf}}{\partial \psi} &= M_f g R_{fcm} (\cos\varphi \sin\theta_2 \cos\psi - \sin\varphi \cos\theta_1 \sin\theta_2 \sin\psi) \\
\frac{\partial U_{gf}}{\partial \theta_2} &= M_f g R_{fcm} (\cos\varphi \cos\theta_2 \cos\psi + \sin\varphi (\cos\theta_1 \cos\theta_2 \cos\psi - \sin\theta_1 \sin\theta_2))
\end{aligned} \tag{B19}$$

References:

Acroname corporation website (2005): http://www.acroname.com/robotics/parts/S1-GP-BRD.html

Halliday, D., Resnick, R., and Walker, J. (2005). Fundamentals of Physics, 7th edition. John Wiley and Sons, Inc., Hoboken, New Jersey.

Harris, A., Stockton, J., Woolery, J., and Ratchford, D. and G.W. Ojakangas (2003). The Orientation Ratchet: A Novel Concept for Producing Net Rotations in Zero Gravity, proposal to the 2003-2004 NASA Reduced Gravity Student Flight Opportunities Program, October, 2003.

Marion, J.B, and S. T. Thornton (1995). Classical mechanics of particles and systems, 4th edition. Thomson Brooks/Cole Publishing, Pacific Grove, CA.

Press, W.H., Teukolsky, S.A., Vetterling, W.T., and B.P. Flannery (1997). Numerical Recipes in FORTRAN 77: The art of scientific computing. Cambridge University Press, Cambridge, England.

Scott, S.H. (1999). Apparatus for measuring and perturbing shoulder and elbow joint positions and torques during reaching, Journal of Neuroscience Methods **89**, 119-127.

Solomon, E.P., Schmidt. R.R., and P.J. Adragna (1990). Human anatomy and physiology, Saunders College Publishing, Philadelphia, PA.

Uno, Y., Kawato, M. and R. Suzuki (1989). Formation and control of optimal trajectory in human multijoint arm movement. Biol. Cybern. **61**, 89-101.

Winter, D.A. (1990). *Biomechanics and motor control of human movement*, 2nd edition, John Wiley and Sons, New York.

Winters, J.M. (1990). Hill-based muscle models: a systems engineering perspective. in *Multiple muscle systems: Biomechanics and movement organization*, Chapter 5, J.M. Winters and S.L.-Y. Woo, (eds), Springer-Verlag.

Zahalak, G.I. (1990). Modeling muscle mechanics and energetics. In *Multiple Muscle Systems: Biomechanics and Movement Organization*, Winters, J.M, and S. L-Y. Woo, eds., Springer-Verlag, New York.

Administrative:

Letter of Endorsement from Drury (see attached)

Letter (Statement?) from supervising faculty (see attached-INSERT?)

Project Costs

The estimated costs for our project are as follows:

- Equipment
  - Skeleton $500
  - Servos $1450
  - LabView Hardware $1500
  - Miscellaneous $200
- *Equipment Total* $*3650*

- Travel
  - Food $1650
  - Car $250
  - Hotel $4000
- *Travel Total* $5800

Project Total: **$9450**

All project costs will be covered by Drury University. Because of this, we see no need for other sources of funding.